Chapter 3

A novel numerical technique for solving nonlinear coupled variable order reaction-diffusion equation

3.1 Introduction

The presence of nonlinear variable order PDE is very important component in the mathematical structure of several complex physical models. It becomes a fascinating notion in fractional calculus when we extend the concept of fractional constant order derivative to time and space dependent fractional derivative. This novel concept of fractional calculus can be used in several characteristics of mechanics, control and signal processing, mathematical physics etc. [93–95]. Finding the numerical solutions of PDE with variable order derivatives are little more complicated in nature than fractional constant order derivatives due to the variable order fractional operators have complex kernels for variable powers. In the article [96], a collocation method based on domain type radial basis function has been applied to a constant and variable order derivatives to find an approximate solution. Chen et al. [97], have presented a new approach of collocation method based on boundary type radial basis function to find the numerical solution of fractional order diffusion equation. To find the numerical solution of variable order fractional differential equation a finite difference scheme has been proposed in [98] along with stability and convergence analyses

of the scheme. Moreover there are many numerical schemes, which have been proposed to find the numerical solutions of variable order fractional differentiation viz., B-linear spline technique, integro quadratic spline interpolation techniques, finite difference method, cubic spline technique, discretization technique, spectral collocation technique etc.

The system of coupled PDEs in porous media describes the interaction and diffusion of two solute species. The dealing with the mathematical models of such physical phenomena is a challenging task. Several systems of coupled PDEs have been discussed in constant fractional order systems viz., KdV-Burgers' equation, Boussinesq-Whitham-Broer-Kaup equation, Burgers' equation, Klein-Gordon -Zakharov equation, etc. These systems have a wide range of applications in many complex physical processes like plasma physics, fluid mechanics, nonlinear wave theory, nonlinear optics, gas dynamics, nonlinear acoustics and shallow water waves, etc.

In this chapter the main aim is to study a special group of nonlinear coupled system of variable order fractional order reaction-diffusion equation. The main motivation behind the concerned coupled PDEs is a vast applications of the model in fluid mechanics, nonlinear optics and nonlinear wave theory, gas dynamics, nonlinear acoustics, and shallow water waves, etc. Many well-known systems of coupled PDEs are the particular cases of the concerned model. The considered variable order coupled system of nonlinear PDEs is given by

$$\begin{aligned}
&\frac{\partial^{\mu_1(x,t)}u(x,t)}{\partial t^{\mu_1(x,t)}} + p_1\frac{\partial^{p_2}u(x,t)}{\partial x^{p_2}} + p_3\frac{\partial^{p_4}v(x,t)}{\partial x^{P_4}} + p_5u(x,t)\frac{\partial u(x,t)}{\partial x} \\
&\qquad\qquad +p_6\frac{\partial(u(x,t)v(x,t))}{\partial x} = h_1(x,t), \\
&\frac{\partial^{\mu_2(x,t)}v(x,t)}{\partial t^{\mu_2(x,t)}} + \tilde{p}_1\frac{\partial^{\tilde{p}_2}u(x,t)}{\partial x^{\tilde{p}_2}} + \tilde{p}_3\frac{\partial^{\tilde{p}_4}v(x,t)}{\partial x^{\tilde{p}_4}} + \tilde{p}_5v(x,t)\frac{\partial v(x,t)}{\partial x} \\
&\qquad\qquad +\tilde{p}_6\frac{\partial(u(x,t)v(x,t))}{\partial x} = h_2(x,t),
\end{aligned} \tag{3.1}$$

with the following initial and boundary conditions

$$\begin{aligned} u(x,0) &= \lambda_1(x), \;\; u(0,t) = \lambda_2(t), \;\; u(1,t) = \lambda_3(t), \\ v(x,0) &= \tilde{\lambda}_1(x), \;\; v(0,t) = \tilde{\lambda}_2(t), \;\; v(1,t) = \tilde{\lambda}_3(t). \end{aligned} \tag{3.2}$$

In the concerned mathematical model (3.1)-(3.2), $u(x,t)$ and $v(x,t)$ are the concentration factors to be determined, $\mu_1(x,t)$ and $\mu_2(x,t)$ denote the variable order derivatives which depend on space and time such that $g-1 < \mu_1(x,t), \mu_2(x,t) < g$. Here g is the first integer not less than $\mu_1(x,t), \mu_2(x,t)$. The other terms $p_{i's}$ and $\tilde{p}_{i's}$ denote some physical realistic constants, $h_1(x,t)$ and $h_2(x,t)$ are the source terms. Here, the another aim is to develop a highly efficient and most powerful technique viz., the operational matrix method based on Bernstein polynomials to find the approximate numerical solution of the considered nonlinear variable order system of a coupled reaction-diffusion equation with given initial and boundary conditions.

3.2 Basic properties and definitions of Bernstein polynomials

Nowadays the Bernstein polynomials are world wide useful in various areas of applied and engineering mathematics[99, 100]. In the unit interval $[0,1]$, Bernstein polynomials of degree l are defined as

$$B_{p,l}(x) = \binom{l}{p} x^p (1-x)^{l-p}, 0 \le p \le l. \tag{3.3}$$

As $0 \le x \le 1$, we can use binomial expansion in the aforementioned equation as

$$B_{p,l}(x) = \binom{l}{p} x^p \Big(\sum_{s=0}^{l-p} (-1)^s \binom{l-p}{s} x^s\Big), 0 \le p \le l, \tag{3.4}$$

or,

$$B_{p,l}(x) = \sum_{s=0}^{l-p} (-1)^s \binom{l}{p} \binom{l-p}{s} x^{p+s}, 0 \leq p \leq l. \tag{3.5}$$

The Bernstein polynomials can be written in the matrix form as

$$\vartheta(x) = MP_l(x), \tag{3.6}$$

where $\vartheta(x) = [B_{0,l}(x), B_{1,l}(x), ..., B_{l,l}(x)]^T$, $P_l(x) = [1, x, x^2, ..., x^l]^T$ and M is an upper triangular matrix given by

$$M = \begin{bmatrix} (-1)^0\binom{l}{0} & (-1)^1\binom{l}{0}\binom{l-0}{1-0} & \dots & \dots & \dots & (-1)^{m-0}\binom{l}{0}\binom{l-0}{1-0} \\ 0 & (-1)^0\binom{l}{1} & \dots & \dots & \dots & (-1)^{m-1}\binom{l}{1}\binom{l-1}{l-1} \\ \vdots & \vdots & \vdots & \vdots & \vdots & \vdots \\ 0 & 0 & \dots & (-1)^0\binom{l}{i} & \dots & (-1)^{m-i}\binom{l}{i}\binom{l-i}{l-i} \\ \vdots & \vdots & \vdots & & \vdots & \vdots \\ 0 & 0 & \dots & \dots & \dots & (-1)^0\binom{l}{l} \end{bmatrix}. \tag{3.7}$$

The format of matrix M reveals that it is an invertible matrix i.e., $|M| \neq 0$. Few properties of Bernstein polynomials are given as follows:

(i) $B_{p,l}(x) \geq 0, \forall x \in [0,1]$ i.e., Bernstein polynomials are always positive in their domain.

(ii) $B_{p,l}(1-x) = B_{l-p,l}(x)$ and (iii) $\tilde{B}_{p,l}(x) = l(B_{p-1,l-1}(x) - B_{p,l-1}(x))$.

3.3 Approximation of the unknown functions

Since the set of Bernstein polynomials forms a complete basis in the Hilbert space $L^2[0,1]$, therefore each function $u(x) \in L^2[0,1]$ can be expressed in terms of Bernstein

polynomials as

$$u(x) \simeq u_r(x) = \sum_{g=0}^{r} b_g B_{g,r}(x) = B^T.\vartheta(x), \tag{3.8}$$

where $B^T = [b_g]$ is the unknown constant matrix, which is known as Bernstein coefficients.

Similarly functions of two variables $u(x,t), v(x,t) \in L^2[0,1]$ can be expressed in terms of Bernstein polynomials as

$$\begin{aligned} u(x,t) \simeq u_r(x,t) &= \sum_{g=0}^{r}\sum_{h=0}^{r} b_{g,h} B_{g,r}(x) B_{h,r}(t) = \vartheta(x)^T.B.\vartheta(t), \\ v(x,t) \simeq v_r(x,t) &= \sum_{g=0}^{r}\sum_{h=0}^{r} \tilde{b}_{i,j} B_{i,r}(x) B_{j,r}(t) = \vartheta(x)^T.\tilde{B}.\vartheta(t), \end{aligned} \tag{3.9}$$

where the unknown constant matrices $B = [b_{g,h}]$ and $\tilde{B} = [\tilde{b}_{i,j}]$ are known as Bernstein coefficients. These coefficients can be determined by using the initial and boundary conditions.

3.4 Operational matrix of the variable order derivative

In this section of the chapter, the operational matrix for the variable order derivative is derived. With the help of equation (3.6), the derivative of the vector $\vartheta(t)$ can be written as

$$\frac{\partial^{\mu(x,t)}\vartheta(t)}{\partial t^{\mu(x,t)}} = \frac{\partial^{\mu(x,t)} M.P_r(t)}{\partial t^{\mu(x,t)}} = M.\frac{\partial^{\mu(x,t)}}{\partial t^{\mu(x,t)}} \begin{bmatrix} 1 \\ t \\ t^2 \\ \vdots \\ t^{g-1} \\ t^g \\ \vdots \\ t^r \end{bmatrix}$$

$$= M. \begin{bmatrix} 0 & 0 & 0 & \dots & 0 & 0 & \dots & 0 & 0 \\ 0 & 0 & 0 & \dots & 0 & 0 & \dots & 0 & 0 \\ 0 & 0 & 0 & \dots & 0 & 0 & \dots & 0 & 0 \\ \vdots & \vdots & \vdots & \vdots & \vdots & \vdots & \vdots & \vdots & \\ 0 & 0 & 0 & \dots & 0 & 0 & \dots & 0 & 0 \\ 0 & 0 & 0 & \dots & 0 & \frac{\Gamma(g+1).t^{-\mu(x,t)}}{\Gamma(g+1-\mu(x,t))} & \dots & 0 & 0 \\ \vdots & \vdots & \vdots & \vdots & \vdots & \vdots & \vdots & \vdots & \vdots \\ 0 & 0 & 0 & \dots & 0 & 0 & \dots & 0 & \frac{\Gamma(r+1).t^{-\mu(x,t)}}{\Gamma(r+1-\mu(x,t))} \end{bmatrix} . \begin{bmatrix} 1 \\ t \\ t^2 \\ \vdots \\ t^{g-1} \\ t^g \\ \vdots \\ t^r \end{bmatrix}, \tag{3.10}$$

where $g-1 \leq \mu(x,t) \leq g$, we take $g = \lceil \mu(x,t) \rceil$ and $g < r$.

From the aforementioned equation, we can write

$$\begin{aligned} \frac{\partial^{\mu(x,t)}\vartheta(t)}{\partial t^{\mu(x,t)}} =& M.\Omega.P_r(t) \\ =& M.\Omega.M^{-1}.\vartheta(t), \end{aligned} \tag{3.11}$$

where Ω is given by the expression

$$\Omega = [a_{pq}]_{(r+1)\times(r+1)} = \begin{cases} 0, & \text{elsewhere,} \\ \frac{\Gamma(g+1).t^{-\mu(x,t)}}{\Gamma(g+1-\mu(x,t))}, & \text{when } p = q \geq g, \end{cases} \tag{3.12}$$

where $M.\Omega.M^{-1}$ is an operational matrix w.r.t. time. The operational matrix for variable order derivatives w.r.t. x can be obtained in a similar manner. Now, by collocating our considered model (3.1), and initial and boundary conditions (3.2), we get a system of nonlinear algebraic equations which help to find the arbitrary constant matrices B and $\tilde{B}$ given in equation (3.9).

3.5 Convergence analysis of the scheme

Theorem: Let the functions $u(x,t), v(x,t) : [0,1] \times [0,1] \longrightarrow \mathbb{R}$ are $(r+1)$ times continuously differentiable functions, i.e., $u, v \in C^{r+1}[0,1]^2$, and let $\mathbb{X} = \text{Span}[B_{p,r}(x), B_{q,r}(t), p, q = 0, 1, ..., r]$ is a vector space. Let $\vartheta(x)^T.B.\vartheta(t)$ and $\vartheta(x)^T.\tilde{B}.\vartheta(t)$ are best approximations of the functions $u(x,t)$ and $v(x,t)$, respectively out of $\mathbb{X}$, then the mean error bounds are given as

$$\begin{aligned} \| u(x,t) - \vartheta(x)^T.B.\vartheta(t) \|_2 &\leq \frac{\sqrt{sc}}{(r+1)!}\frac{r+2}{2^{2r+4}}, \\ \| v(x,t) - \vartheta(x)^T.\tilde{B}.\vartheta(t) \|_2 &\leq \frac{\sqrt{\tilde{s}c}}{(r+1)!}\frac{r+2}{2^{2r+4}}, \end{aligned} \tag{3.13}$$

where $s = max[s_0, s_1, ..., s_{r+1}]$, $\tilde{s} = max[\tilde{s}_0, \tilde{s}_1, ..., \tilde{s}_{r+1}]$ and

$c = max[\binom{r+1}{a}, 0 \leq a \leq r+1]$.

Proof: The Taylor series approximation of the function $u(x,t)$ in the neighborhood

of a point (x_0, t_0) is given by

$$u_r(x,t) = u(x_0,t_0) + u_x^{'}(x_0,t_0)(x-x_0) + u_t^{'}(x_0,t_0)(t-t_0) + \cdots , \tag{3.14}$$

from which we can obtain

$$\mid u(x,t) - u_r(x,t) \mid = \mid \frac{1}{(r+1)!} \sum_{a=0}^{r+1} \binom{r+1}{a} u^{r+1}_{x^{r+1-a}t^a}(x_0,t_0)(x-x_0)^{r+1-a}(t-t_0)^a \mid . \tag{3.15}$$

Suppose that $\vartheta(x)^T.B.\vartheta(t)$ be the best approximation of $u(x,t)$, then

$$\parallel u(x,t) - \vartheta(x)^T.B.\vartheta(t) \parallel_2^2 \leq \parallel u(x,t) - u_r(x,t) \parallel_2^2 = \int_0^1 \int_0^1 \mid u(x,t) - u_r(x,t) \mid^2 dxdt. \tag{3.16}$$

In view of equation (3.15), we have

$$\begin{aligned} \parallel u(x,t) - \vartheta(x)^T.B.\vartheta(t) \parallel_2^2 \leq \int_0^1 \int_0^1 \mid \frac{1}{(r+1)!} \sum_{a=0}^{r+1} \binom{r+1}{a} u^{r+1}_{x^{r+1-a}t^a}(x_0,t_0) \\ (x-x_0)^{r+1-a}(t-t_0)^a \mid^2 dxdt. \end{aligned} \tag{3.17}$$

It is assumed that $u^{r+1}_{x^{r+1-a}t^a}(x,t)$ is $(r+1)$ times continuously differentiable function, therefore there exist constants $s_0, s_1, ..., s_{r+1}$ such that

$$\underset{0 \leq x,t \leq 1}{max}\, u^{r+1}_{x^{r+1-a}t^a}(x,t) \leq s_a, 0 \leq a \leq r+1. \tag{3.18}$$

Now we have

$$\begin{aligned} \parallel u(x,t) - \vartheta(x)^T.B.\vartheta(t) \parallel_2^2 \leq \int_0^1 \int_0^1 \mid \frac{1}{(r+1)!} \sum_{a=0}^{r+1} \binom{r+1}{a} s_a (x-x_0)^{r+1-a} \\ (t-t_0)^a \mid^2 dxdt. \end{aligned} \tag{3.19}$$

Considering $s = max[s_0, s_1, ..., s_{r+1}]$ and $c = max[\binom{r+1}{a}, 0 \leq a \leq r+1]$, the equation (3.19), becomes

$$\| u(x,t) - \vartheta(x)^T.B.\vartheta(t) \|_2^2 \leq \frac{sc}{(r+1)!^2} \int_0^1 \int_0^1 | \sum_{a=0}^{r+1} (x-x_0)^{r+1-a}(t-t_0)^a |^2 \, dxdt. \tag{3.20}$$

Suppose that y_j be the roots of Bernstein Polynomials. For the term $(x-x_0)^{r+1-a}$ one can find the following bounds by using the mapping $x = \frac{y+1}{2}$ between the intervals [-1,1] and [0,1] as

$$\min_{0\leq x_j\leq 1} \max_{0\leq x\leq 1} | (x-x_0)^{r+1-a} | = \min_{0\leq y_j\leq 1} \max_{0\leq y\leq 1} | (\frac{y-y_j}{2})^{r+1-a} | = \frac{1}{2^{2(r+1-a)+1}}. \tag{3.21}$$

Thus form the equation (3.20), we can write

$$\| u(x,t) - \vartheta(x)^T.B.\vartheta(t) \|_2^2 \leq \frac{sc}{(r+1)!^2} \int_0^1 \int_0^1 | \sum_{a=0}^{r+1} \frac{1}{2^{2(r+1-a)+1}} \frac{1}{2^{2a+1}} |^2 \, dxdt, \tag{3.22}$$

or,

$$\| u(x,t) - \vartheta(x)^T.B.\vartheta(t) \|_2^2 \leq \frac{sc}{(r+1)!^2} \frac{(r+2)^2}{2^{4r+8}}. \tag{3.23}$$

Now taking the square root on both sides of above equation we get our desired error bound. Similarly, the error bound for $v(x,t)$ can be calculated.

3.6 Numerical simulations and error analysis

In this section, the operational matrix method based on Bernstein polynomials has been applied to some nonlinear variable order coupled PDEs to show the efficiency and accuracy of the proposed numerical scheme through error analysis. The software Mathematica 11.3 is used for whole numerical computation. The amount of time taken by the program code for numerical outputs in Mathematica 11.3 increases

slowly as the order of approximation r is increased, i.e., time complexity increases with the increase in order of approximation.

Example 1: Coupled Whitham-Broer-Kaup (WBK) Equations: Consider the following nonlinear variable order coupled reaction-diffusion equation as

$$\begin{aligned} &\frac{\partial^{\mu_1(x,t)}u(x,t)}{\partial t^{\mu_1(x,t)}} + \frac{\partial^2 u(x,t)}{\partial x^2} + \frac{\partial v(x,t)}{\partial x} + u(x,t)\frac{\partial u(x,t)}{\partial x} = h_1(x,t), \\ &\frac{\partial^{\mu_2(x,t)}v(x,t)}{\partial t^{\mu_2(x,t)}} + \frac{\partial^3 u(x,t)}{\partial x^3} - \frac{\partial^3 v(x,t)}{\partial x^3} + \frac{\partial(u(x,t)v(x,t))}{\partial x} = h_2(x,t). \end{aligned} \tag{3.24}$$

This system of PDE explains many physical phenomenon arising in fluid mechanics. This equation is known as system of coupled Whitham-Broer-Kaup (WBK) equations. The analytical solutions of this coupled system are $u(x,t) = \frac{4}{1+exp(2(x-3t))}$ and $v(x,t) = \frac{3exp(2(x-3t))}{(1+exp(2(x-3t)))^2}$ with suitable values of $h_1(x,t)$ and $h_2(x,t)$. The initial and boundary conditions can be derived from the exact solution of the problem. The L_2 norm error and L_∞ normed errors between the exact solutions and the solutions obtained by our proposed method defined in equations (2.25) and (2.26), respectively are shown through Table 3.1 and Table 3.2 for different values of fractional orders $\mu_1(x,t)$ and $\mu_2(x,t)$, respectively at different values of time t and for different order of approximation r. We can easily found the fact that these errors decrease as the order of approximation increases. This error analysis shows the high efficiency of proposed numerical scheme during the computation of numerical solution. Hence comparing the numerical solution and exact solution, one can ensure the effectiveness and efficiency of the proposed numerical scheme.

TABLE 3.1: Comparison of L_∞ and L_2 norm errors for $u(x,t)$ at $t = 0.05$

	$\mu_1(x,t) = \frac{e^{-t}\cos x}{400}$		$\mu_1(x,t) = \frac{2\cos x+\sin t}{400}$		$\mu_1(x,t) = \frac{\sin t+e^{-t}\cos x}{300}$	
r	L_∞	L_2	L_∞	L_2	L_∞	L_2
4	5.23×10^{-10}	5.42×10^{-10}	5.98×10^{-10}	6.04×10^{-10}	6.24×10^{-10}	6.43×10^{-10}
5	6.73×10^{-12}	6.92×10^{-12}	2.29×10^{-12}	5.53×10^{-11}	3.67×10^{-11}	6.83×10^{-11}
6	4.20×10^{-13}	8.83×10^{-13}	3.18×10^{-13}	7.64×10^{-13}	7.46×10^{-13}	8.37×10^{-12}
7	1.09×10^{-16}	5.64×10^{-15}	2.78×10^{-16}	4.00×10^{-16}	4.64×10^{-16}	1.02×10^{-15}

TABLE 3.2: Comparison of L_∞ and L_2 norm errors for $v(x,t)$ at $t = 0.05$

	$\mu_2(x,t) = \frac{e^{-t}\cos x}{400}$		$\mu_2(x,t) = \frac{2\cos x+\sin t}{400}$		$\mu_2(x,t) = \frac{\sin t+e^{-t}\cos x}{300}$	
r	L_∞	L_2	L_∞	L_2	L_∞	L_2
4	5.34×10^{-10}	8.23×10^{-10}	4.24×10^{-10}	5.30×10^{-10}	9.94×10^{-10}	3.03×10^{-09}
5	1.39×10^{-12}	4.54×10^{-12}	4.39×10^{-12}	5.84×10^{-12}	6.43×10^{-12}	5.34×10^{-11}
6	4.34×10^{-14}	1.09×10^{-13}	1.54×10^{-13}	4.63×10^{-13}	2.12×10^{-13}	4.03×10^{-13}
7	6.33×10^{-16}	7.40×10^{-16}	3.53×10^{-16}	1.43×10^{-15}	1.64×10^{-16}	5.32×10^{-16}

Example 2: Coupled KdV-Burgers Equations: Consider a particular case of the model (3.1), which is the following nonlinear variable order coupled reaction-diffusion equation

$$\begin{aligned} \frac{\partial^{\mu_1(x,t)}u(x,t)}{\partial t^{\mu_1(x,t)}} + \frac{\partial^3 u(x,t)}{\partial x^3} + \frac{\partial^2 v(x,t)}{\partial x^2} + u(x,t)\frac{\partial u(x,t)}{\partial x} = h_1(x,t), \\ \frac{\partial^{\mu_2(x,t)}v(x,t)}{\partial t^{\mu_2(x,t)}} + \frac{\partial^3 u(x,t)}{\partial x^3} + \frac{\partial^2 v(x,t)}{\partial x^2} + v(x,t)\frac{\partial v(x,t)}{\partial x} = h_2(x,t). \end{aligned} \tag{3.25}$$

This system of coupled PDE describes several physical phenomena arising in nonlinear optics and nonlinear wave theory. This system is known as system of coupled KdV-Burgers Equations. The analytical solutions of this coupled system are $u(x,t) = exp(x+t)\sin(xt)$ and $v(x,t) = exp(x+t)\cos(xt)$ with suitable values of $h_1(x,t)$ and $h_2(x,t)$. The error analysis through the comparison of L_2 and L_∞ is shown through the Table 3.3 and Table 3.4 for different values of fractional order

$\mu_1(x,t)$ and $\mu_2(x,t)$, respectively for various values of t and r. We can easily found the fact that these errors decreases as the order of approximation increases. This error analysis shows the high efficiency and accuracy of proposed numerical scheme during the computation of numerical solution.

TABLE 3.3: Comparison of L_∞ and L_2 norm errors for $u(x,t)$ at $t = 0.05$

	$\mu_1(x,t) = \frac{\cos t + e^{-2t}\sin x}{300}$		$\mu_1(x,t) = \frac{e^{-2t}\sin x}{400}$		$\mu_1(x,t) = \frac{\sin t + e^{-t}\cos x}{400}$	
r	L_∞	L_2	L_∞	L_2	L_∞	L_2
4	1.06×10^{-10}	2.13×10^{-10}	2.74×10^{-10}	7.75×10^{-10}	6.86×10^{-10}	8.63×10^{-10}
5	3.76×10^{-11}	4.86×10^{-11}	4.86×10^{-11}	5.84×10^{-11}	1.53×10^{-11}	5.95×10^{-11}
6	7.54×10^{-13}	8.26×10^{-13}	5.85×10^{-13}	7.28×10^{-12}	5.86×10^{-13}	7.73×10^{-13}
7	9.86×10^{-15}	9.94×10^{-15}	2.96×10^{-15}	4.86×10^{-15}	1.56×10^{-15}	8.86×10^{-14}

TABLE 3.4: Comparison of L_∞ and L_2 norm errors for $v(x,t)$ at $t = 0.05$

	$\mu_2(x,t) = \frac{\cos t + e^{-2t}\sin x}{300}$		$\mu_2(x,t) = \frac{e^{-2t}\sin x}{400}$		$\mu_2(x,t) = \frac{\sin t + e^{-t}\cos x}{400}$	
r	L_∞	L_2	L_∞	L_2	L_∞	L_2
4	7.93×10^{-10}	7.98×10^{-10}	4.32×10^{-10}	6.42×10^{-10}	1.02×10^{-10}	1.64×10^{-10}
5	6.41×10^{-11}	4.32×10^{-10}	4.22×10^{-11}	8.94×10^{-11}	6.42×10^{-11}	8.43×10^{-11}
6	4.32×10^{-13}	6.34×10^{-12}	8.53×10^{-13}	9.64×10^{-13}	5.75×10^{-13}	7.33×10^{-13}
7	6.48×10^{-15}	3.42×10^{-14}	6.34×10^{-15}	7.53×10^{-15}	1.53×10^{-15}	6.34×10^{-15}

Example 3: Coupled Burgers Equation: Here a particular case of the model (3.1) is Considered as

$$\begin{aligned} &\frac{\partial^{\mu_1(x,t)}u(x,t)}{\partial t^{\mu_1(x,t)}} - \frac{\partial^2 u(x,t)}{\partial x^2} - 2u(x,t)\frac{\partial u(x,t)}{\partial x} + \frac{\partial(u(x,t)v(x,t))}{\partial x} = h_1(x,t), \\ &\frac{\partial^{\mu_2(x,t)}u(x,t)}{\partial t^{\mu_2(x,t)}} - \frac{\partial^2 v(x,t)}{\partial x^2} - 2v(x,t)\frac{\partial v(x,t)}{\partial x} + \frac{\partial(u(x,t)v(x,t))}{\partial x} = h_2(x,t). \end{aligned} \tag{3.26}$$

This system of coupled PDE has wide range of application in several physical phenomena like fluid mechanics, gas dynamics, nonlinear acoustics. This equation is

known as system of coupled Burgers Equation. The analytical solutions of this coupled system are $u(x,t) = e^{-t}\sin x$ and $v(x,t) = e^{-t}\sin x$ with suitable values of $h_1(x,t)$ and $h_2(x,t)$.

The error analysis through the comparison of L_2 and L_∞ is shown through Table 3.5 and Table 3.6 for different values of $\mu_1(x,t)$ and $\mu_2(x,t)$, respectively for different values of t and r. It is seen that the errors decrease as the order of approximation increases. This error analysis shows the high efficiency of the proposed numerical scheme during the computation of numerical solution.

TABLE 3.5: Comparison of L_∞ and L_2 norm errors for $u(x,t)$ at $t = 0.05$

	$\mu_1(x,t) = \frac{2\cos t + e^{-2t}\sin 2x}{300}$		$\mu_1(x,t) = \frac{2e^{-2t}\cos x}{400}$		$\mu_1(x,t) = \frac{\sin 2t + 2e^{-t}\cos x}{400}$	
r	L_∞	L_2	L_∞	L_2	L_∞	L_2
4	9.02×10^{-10}	1.83×10^{-09}	2.56×10^{-10}	4.38×10^{-10}	1.17×10^{-10}	4.27×10^{-10}
5	5.26×10^{-11}	8.51×10^{-11}	1.03×10^{-11}	4.32×10^{-11}	2.14×10^{-11}	4.63×10^{-11}
6	1.86×10^{-13}	3.94×10^{-13}	7.54×10^{-14}	1.76×10^{-13}	6.86×10^{-13}	5.43×10^{-12}
7	5.34×10^{-16}	6.45×10^{-16}	5.04×10^{-16}	3.85×10^{-15}	7.54×10^{-16}	9.54×10^{-15}

TABLE 3.6: Comparison of L_∞ and L_2 norm errors for $v(x,t)$ at $t = 0.05$

	$\mu_2(x,t) = \frac{2\cos t + e^{-2t}\sin 2x}{300}$		$\mu_2(x,t) = \frac{2e^{-2t}\cos x}{400}$		$\mu_2(x,t) = \frac{\sin 2t + 2e^{-t}\cos x}{400}$	
r	L_∞	L_2	L_∞	L_2	L_∞	L_2
4	1.75×10^{-10}	7.58×10^{-10}	1.65×10^{-10}	8.56×10^{-10}	8.98×10^{-10}	9.48×10^{-10}
5	4.42×10^{-12}	1.49×10^{-11}	4.04×10^{-12}	9.71×10^{-11}	6.43×10^{-11}	9.73×10^{-11}
6	7.95×10^{-13}	1.03×10^{-13}	7.53×10^{-13}	8.09×10^{-13}	5.81×10^{-13}	8.41×10^{-12}
7	5.73×10^{-15}	6.75×10^{-15}	3.90×10^{-15}	1.86×10^{-14}	1.62×10^{-15}	9.76×10^{-15}

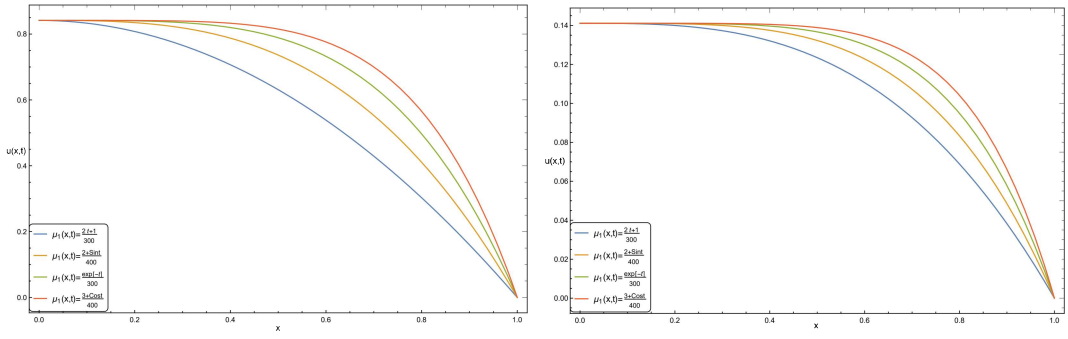

(a) (b)

FIGURE 3.1: Plots of $u(x,t)$ vs. x for different fractional variable order for (a) $p_1 = -1$, (b) $p_1 = 1$.

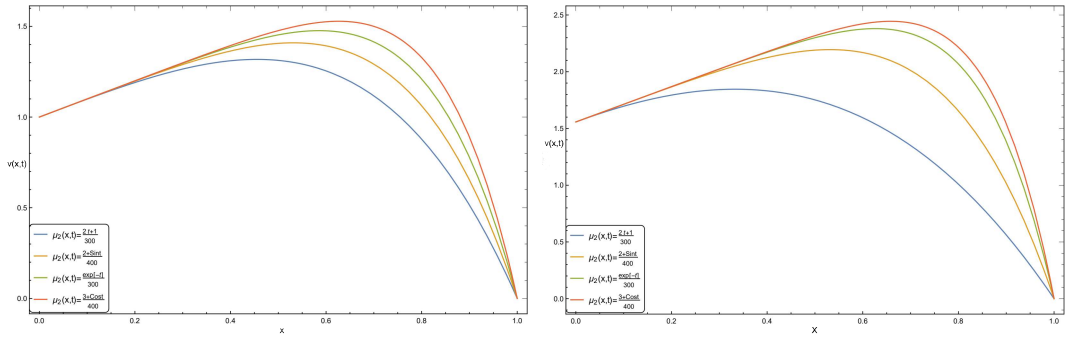

(a) (b)

FIGURE 3.2: Plots of $v(x,t)$ vs. x for different fractional variable order for (a) $\tilde{p}_3 = 1$, (b) $\tilde{p}_3 = -1$.

3.7 Results and discussion

After the validation of the efficiency of the proposed numerical method which applying it on three given examples in the previous section, the author has made an endeavour to apply in the considered mathematical model (3.1) for different particular values of the parameters taking $h_1(x,t) = 0 = h_2(x,t)$. The behavior of solute concentration for different variable order is shown in the following figures for different values of constant coefficients.

The overshoots of solute profiles $u(x,t)$ and $v(x,t)$ for different variable orders

$\mu_1(x,t)$ and $\mu_2(x,t)$ at $t = 1$ are shown through the Figures 3.1-3.2. Figures 3.1(a) and 3.1(b) are the plots of solute profile $u(x,t)$ vs. spatial variable x for $p_1 = 1$ and $p_1 = -1$, respectively when other constant coefficients are taken as $p_2 = 1.2 = p_4 = \tilde{p}_2 = \tilde{p}_4, p_3 = 1 = p_5 = p_6 = \tilde{p}_1 = \tilde{p}_3 = \tilde{p}_5 = \tilde{p}_6$. Figures 3.2(a) and 3.2(b) are the plots of solute profile $v(x,t)$ vs. spatial variable x for $\tilde{p}_3 = 1$ and $\tilde{p}_3 = -1$, respectively when other constant coefficients are taken as $p_2 = 1.2 = p_4 = \tilde{p}_2 = \tilde{p}_4, p_1 = 1 = p_3 = p_5 = p_6 = \tilde{p}_1 = \tilde{p}_5 = \tilde{p}_6$. The effects of advection term are also justified from variation of the solute profile variations as shown in the said figures.

3.8 Conclusion

Present chapter provides three useful consequences. The first one is the derivation of Bernstein operational matrices of variable order derivatives w.r.t. space and time. The second one is the proper utilization of collocation method with the Bernstein polynomial to solve the nonlinear variable order coupled system of reaction-diffusion equation with the prescribed initial and boundary conditions and the third one is finding the stability analysis and error bounds for the approximation and demonstration of error analysis. Overshoots of solute concentration have also been justified in the chapter. The author is optimist that in future, the proposed efficient technique can be applied to solve more complex physical models like two-dimensional nonlinear variable order advection-reaction-diffusion and a two-dimensional variable order coupled system of equations.

****